

PAPER • OPEN ACCESS

Simulation of 2D Brain's Potential Distribution Based on Two Electrodes ECVT Using Finite Element Method

To cite this article: S H Sirait *et al* 2016 *J. Phys.: Conf. Ser.* **739** 012126

View the [article online](#) for updates and enhancements.

Related content

- [Characterization of a multi-plane electrical capacitance tomography sensor with different numbers of electrodes](#)
Jiamin Ye, Haigang Wang and Wuqiang Yang
- [ECVT with high contrast dielectrics](#)
Mark A Nurge
- [Approximation of a norm-preserving gradient flow](#)
Qiang Du and Fanghua Lin



IOP | ebooks™

Bringing together innovative digital publishing with leading authors from the global scientific community.

Start exploring the collection—download the first chapter of every title for free.

Simulation of 2D Brain's Potential Distribution Based on Two Electrodes ECVT Using Finite Element Method

S H Sirait¹, R E Edison², M R Baidillah², W P Taruno² and F Haryanto¹

¹ Nuclear Physics and Biophysics Division, Physics Department Institut Teknologi Bandung, Indonesia

² CTECH Labs Edwar Technology, Tangerang, Indonesia

E-mail: syarif.hussein.sirait@gmail.com

Abstract. The aim of this study is to simulate the potential distribution of 2D brain geometry based on two electrodes ECVT. ECVT (electrical capacitance tomography) is a tomography modality which produces dielectric distribution image of a subject from several capacitance electrodes measurements. This study begins by producing the geometry of 2D brain based on MRI image and then setting the boundary conditions on the boundaries of the geometry. The values of boundary conditions follow the potential values used in two electrodes brain ECVT, and for this reason the first boundary is set to 20 volt and 2.5 MHz signal and another boundary is set to ground. Poisson equation is implemented as the governing equation in the 2D brain geometry and finite element method is used to solve the equation. Simulated Hodgkin-Huxley action potential is applied as disturbance potential in the geometry. We divide this study into two which comprises simulation without disturbance potential and simulation with disturbance potential. From this study, each of time dependent potential distributions from non-disturbance and disturbance potential of the 2D brain geometry has been generated.

1. Introduction

Brain is an important organ in the human body. The brain basically serves to regulate and coordinate most of the movement, behavior and homeostatic of body functions, such as heart, blood pressure, and body temperature. The human brain is responsible for setting the whole body and the way human think. Studying the brain is important so that human can improve their health quality. One method to learn the brain is to use tomography modality. As the brain is important for the body, a tomography modality for the brain should be safe, non-invasive, and accurate.

Recently, ECVT as a new tomography modality has been used in medical physics field to study human brain functions [1] and human brain activity [2]. ECVT (electrical capacitance volume tomography) is a tomography modality for direct volume imaging of permittivity distributions based on utilizing capacitance sensor. ECVT is a system developed based on ECT (electrical capacitance tomography) constructing the 2D permittivity distribution. In the beginning of its development, ECVT is used in industrial processes for dynamic flow imaging because of its capabilities to reconstruct image in real time, non-invasive, and non-destructive. ECVT system consists of three parts: (1) sensor, (2) data acquisition system, and (3) a computer system for reconstruction and viewing reconstructed images.



In general ECVT system has two problems: (1) forward problem, and (2) inverse problem to produce the final result [3]. Forward problem includes task of collecting capacitance data from sensors placed around the wall which could be studied either by a simulation or a direct measurements with capacitance sensors. Inverse problem includes task of reconstructing permittivity distributions image from the collected capacitance data. Studies in inverse problems, which are about image reconstruction using appropriate algorithms, have been commonly reported in industrial ECVT [3, 4] and in brain ECVT [1, 2] due to its similar principles. However, studies in forward problem specifically in brain ECVT are less known until now.

In this paper, we study forward problem of ECVT on 2D brain geometry by simulation using finite element method based on two brain ECVT electrodes. In ECVT, finite element method resolves the potential distribution in the domain, and then it calculates the capacitance values in it. However, to analyze the parameters which are changing the brain capacitance, we could study it from the potential distribution on the geometry. Therefore, in this paper we only study the potential distribution in geometry produced by finite element method.

2. Methodology

The methods of this study begin with designing two electrodes brain ECVT sensor. In general ECVT includes 8 or 32 electrodes sensor, but in this study we only use two sensors because two sensors is adequate for generating the brain potential distribution. Sensor design is based on the design of 2D ECT sensor (Electrical Capacitance Tomography) [5] shown in figure 1 (a). An ECT sensor consists of several electrodes mounted on outside of a vessel, and it is surrounded by a guard screen. The guard screen on the outer side of the sensor is set to ground to reduce the effects of external electric fields. Axial screens are mounted between electrodes to avoid the electric field from excitation electrode reaching detector electrode directly without being influenced by dielectric object in geometry.

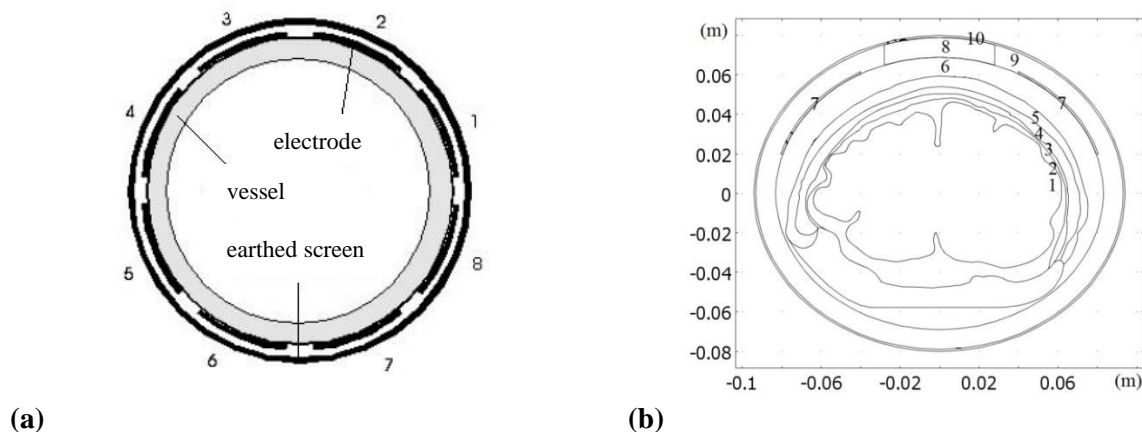


Figure 1. (a) Sensor design, (b) MRI based 2D coronal brain geometry and sensor

The 2D coronal brain geometry merged with sensor design is shown in figure 1 (b). The 2D brain's geometry structure is produced based on MRI image, and it is segmented into five tissue types following the simulation done by Miranda [6]. The brain is assumed has isotropic physical properties based on simulation by Miranda [6]. From inside to outside, the brain geometry consists of white matter, grey matter, CSF, skull, skin, and vessel with each of its relative permittivity at 2.5MHz are 308, 604, 109, 93, 799, and 3 respectively [7]. Two electrodes ($\epsilon_r = 1$) with 5cm length and 5cm width showed in number seven on figure 1 (b) are positioned outside the vessel. From figure 1 (b), number seven on left side depicts excitation electrode, and number seven on right side depicts detector electrode. Number eight depicts axial screen, and number nine depicts air layer.

In real, brain ECVT applies electrical sinusoidal signal with 20 volt voltage and 2.5MHz frequency. For the governing equation in the geometry, Poisson equation is implemented, and

electrostatic approximation is chosen as described in ECT [8, 9, 10] and ECVT [3, 4]. This electrostatic approximation is chosen with assuming that there are no magnetic fields in domain so that $\nabla \times E = 0$. Because the domain length ($\approx 0.2\text{m}$) is tinier than the wave length ($\approx 100\text{m}$), there are no waves propagation happens. With assuming there are no free charges existed in brain geometry, the equation of the brain ECVT and the boundary condition become:

$$\begin{aligned}\nabla \cdot (\epsilon \nabla V) &= 0 \\ V|_{\Gamma_i} &= V; V|_{\Gamma_j} = 0\end{aligned}\quad (1)$$

with $V = 20\sin(2\pi(2.5\text{MHz})t)$ volt. Both Γ_i and Γ_j are boundary condition for excitation electrode and detection electrode respectively. In this study time interval is $1 \times 10^{-7}\text{s}$.

As potential disturbance, simulated Hodgkin-Huxley action potential is applied. Simulated Hodgkin-Huxley action potential is shown in figure 2. We put this potential at (0, 2.3) in brain layer with assuming that there are electrical activities in white matter.

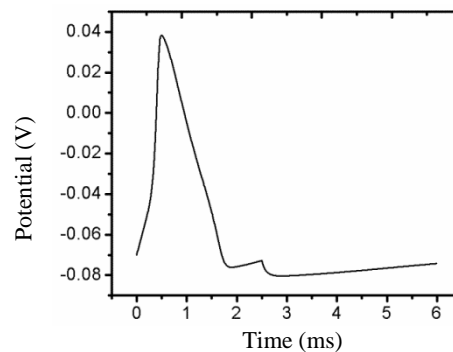


Figure 2. Simulated Hodgkin-Huxley Action Potential

The forward problem in ECVT is the problem of calculating the potential distribution with solving the implemented governing equation. After that, it calculates the capacitance value on the geometry using the potential distribution which already known. Finite element method works with discretizing the geometry into small elements such as triangle, or tetrahedral. These elements contain nodes and edges. For solving the governing equation, finite element changes the differential equation into weak form. So the equation 1 in 2D becomes:

$$-\int_{\Omega} \nabla w \cdot \mathbf{D} dA = -\int_{\Gamma} w \mathbf{D} \cdot \mathbf{n} dl \quad (2)$$

with w is weighted residual and \mathbf{D} is electric displacement.

3. Results and Discussion

These simulations use coronal slice of brain consisting of five layers. Domain is discretized using triangle elements. Based on figure 3, the domain has been successfully discretized and has 25297 elements.

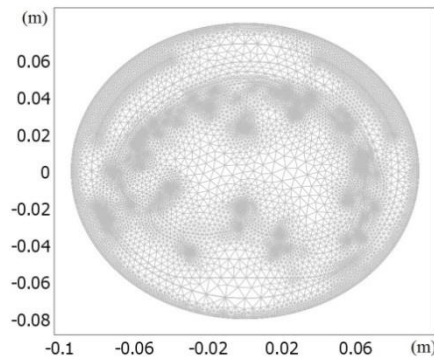


Figure 3. Discretization of the geometry

The potential distributions are divided into two parts, i.e., without disturbance potential and with disturbance potential. We put profile picture to each of potential distributions image to simplify the potential inspection. In profile picture, the excitation electrode is laid around -8cm in x-axis, the detector electrode is laid around 8cm in x-axis, and brain layer is laid from -6cm to 6cm in x-axis. The disturbance potential is located in 0cm in x-axis and 2.3 in y-axis. The time dependent potential distributions are divided into four parts i.e. at 0s, 1×10^{-7} s, 2×10^{-7} s, and 3×10^{-7} s for one cycle sinusoidal signal with 2.5MHz frequency.

3.1. Without disturbance potential

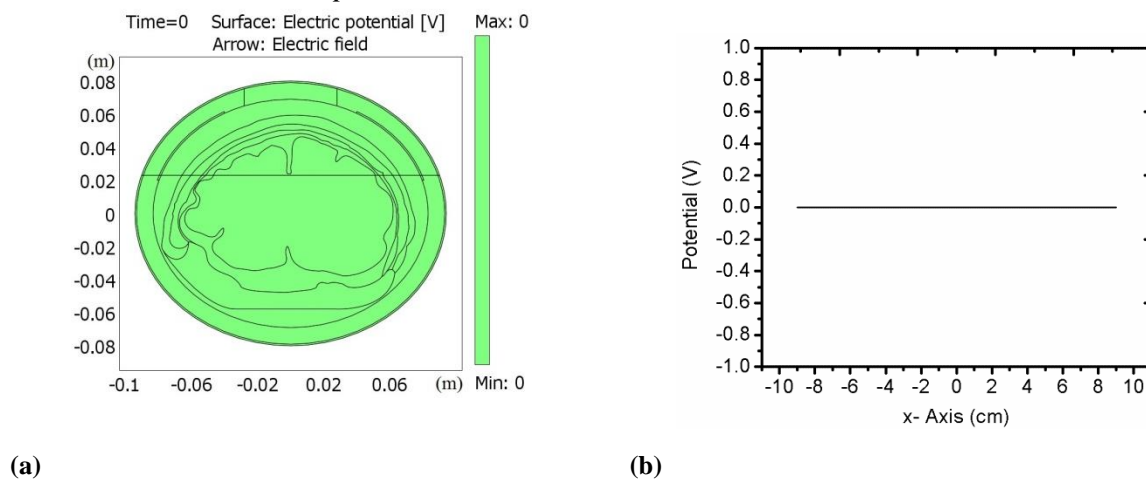


Figure 4. (a) Potential distribution without disturbance at $t = 0$ s,
(b) Profile of potential distribution

Figure 4 (a) is potential distribution without potential disturbance at 0s. Figure 4 (b) is profile of potential distribution in figure 4 (a). At this time, the signal excitation is still 0 volt. From figure 4 (b), it is clear that the whole geometry is still around 0 volt because there is no potential in excitation electrode at this time.

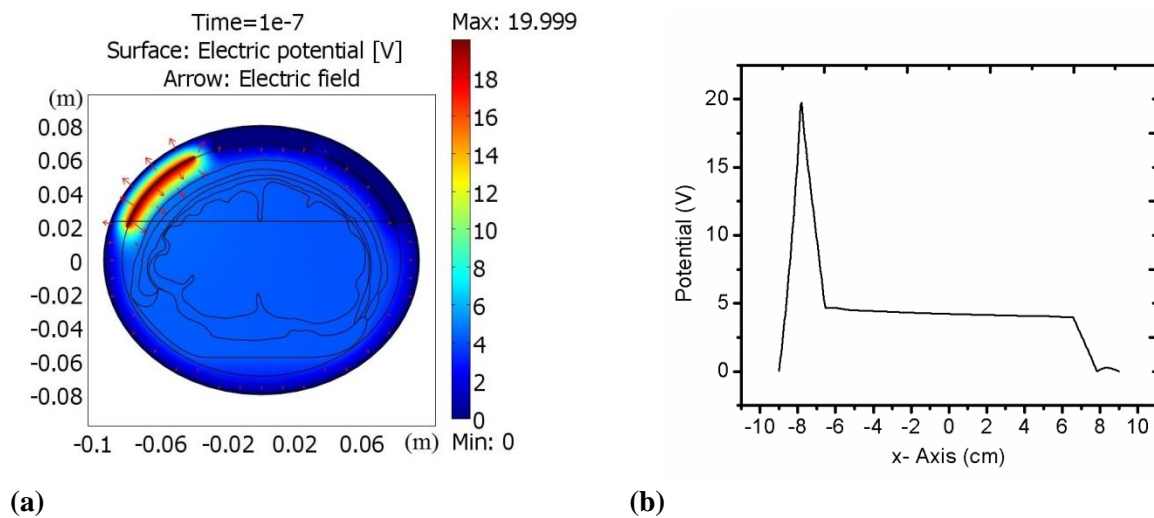


Figure 5. (a) Potential distribution without disturbance at $t = 1 \times 10^{-7}$ s,
(b) Profile of potential distribution

Figure 5 (a) is potential distribution in geometry at 1×10^{-7} s. At this time, the signal excitation reaches 20 volt. Figure 5 (b) shows that the potential around excitation electrode is about 20 volt, and the potential around detector electrode is about 0 volt. There is a sharp decrease in potential distribution between excitation electrode position and brain layer position from around 20 volt to under 5 volt before remaining stable in the brain layers, and then it declines significantly to around 0 volt in detection electrode.

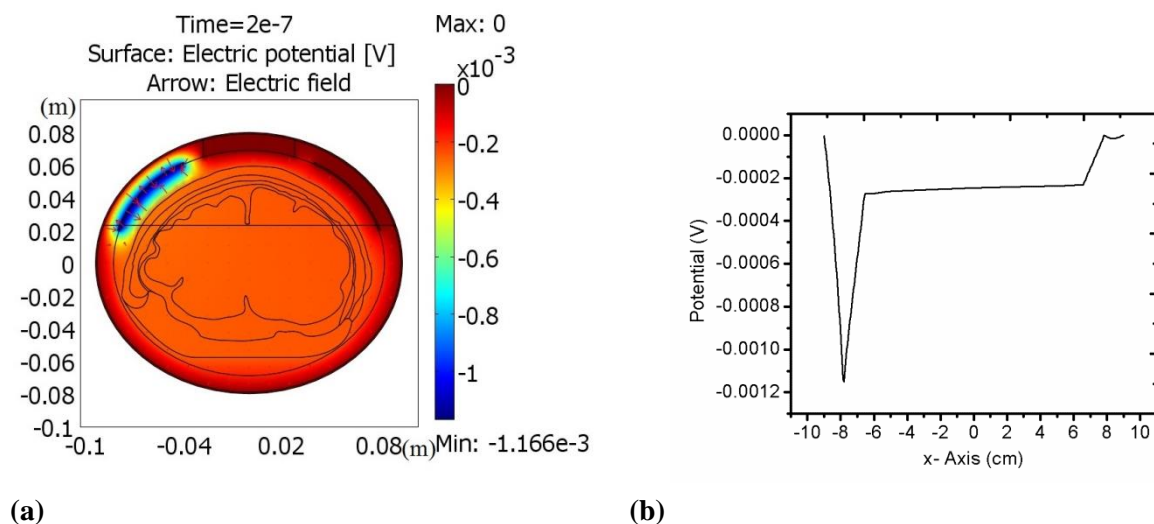


Figure 6. (a) Potential distribution without disturbance at $t = 2 \times 10^{-7}$ s,
(b) Profile of potential distribution

Figure 6 (a) is potential distribution in geometry at 2×10^{-7} s. At this time, the signal excitation backs to about 0 volt. Figure 6 (b) shows that the potential around excitation electrode is about -0.0012 volt which is tiny, and the potential around detector electrode is about 0 volt. The pattern is similar to potential distribution at 1×10^{-7} s, but it has smaller amount and the sign oppose each other.

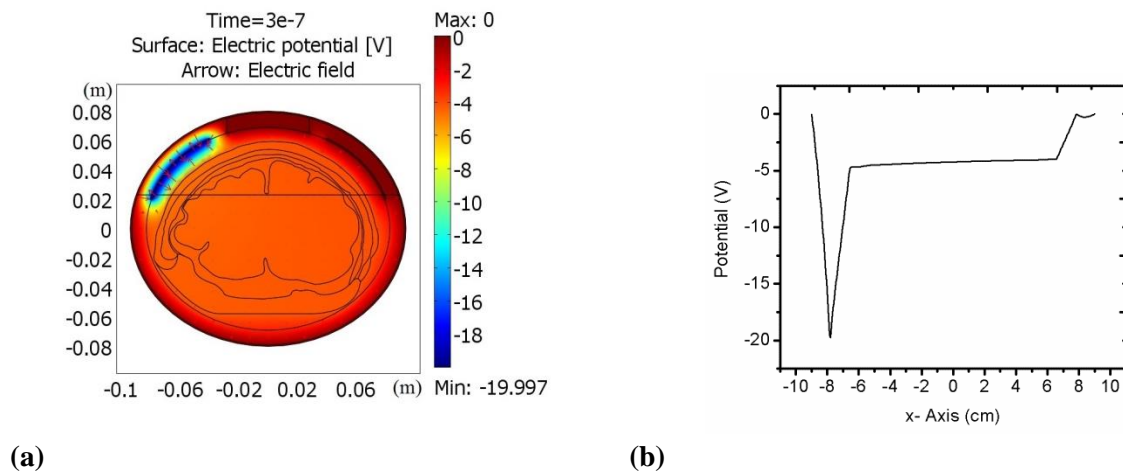


Figure 7. (a) Potential distribution without disturbance at $t = 3 \times 10^{-7}$ s,
(b) Profile of potential distribution

Figure 7 (a) is potential distribution in geometry at 3×10^{-7} s. At this time, the signal excitation reaches -20 volt. Figure 7 (b) shows that the potential around excitation electrode is about -20 volt, and the potential around detector electrode is about 0 volt. This result is similar to result at $t = 1 \times 10^{-7}$ s except its sign oppose each other.

3.2. With disturbance potential

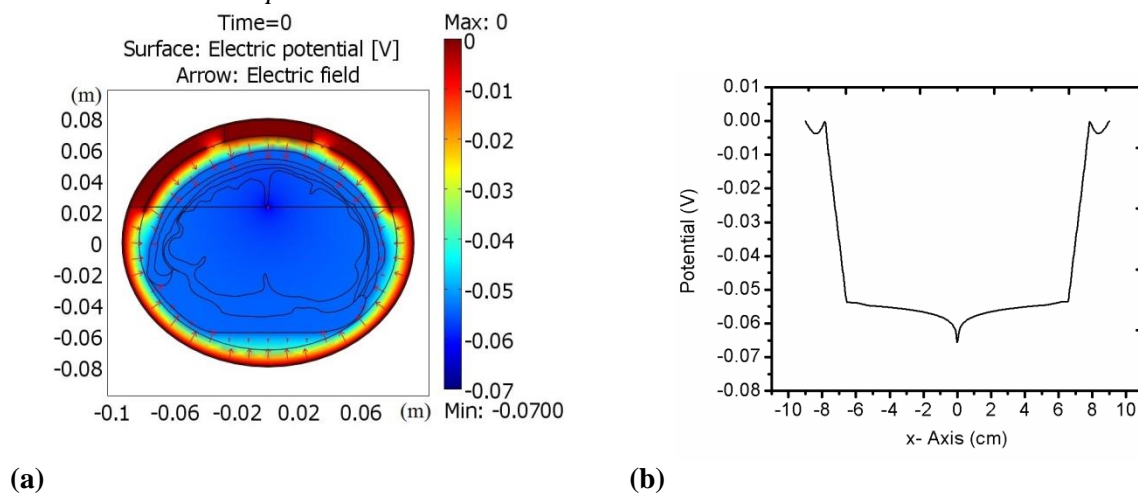


Figure 8. (a) Potential distribution with disturbance at $t = 0$ s,
(b) Profile of potential distribution

Figure 8 (a) is picture for potential distribution with simulated hodgkin-huxley action potential applied as potential disturbance on the brain geometry. From figure 8 (a), we can see the position of disturbance potential is at (0, 2.3) as a black color point. At this time, the signal excitation is still zero volt. Figure 8 (b) shows that the potential around excitation electrode and detector electrode are about 0 volt. Potential in brain layer is around -0.05 volt, and it decreases slightly to about -0.07 volt at disturbance potential position.

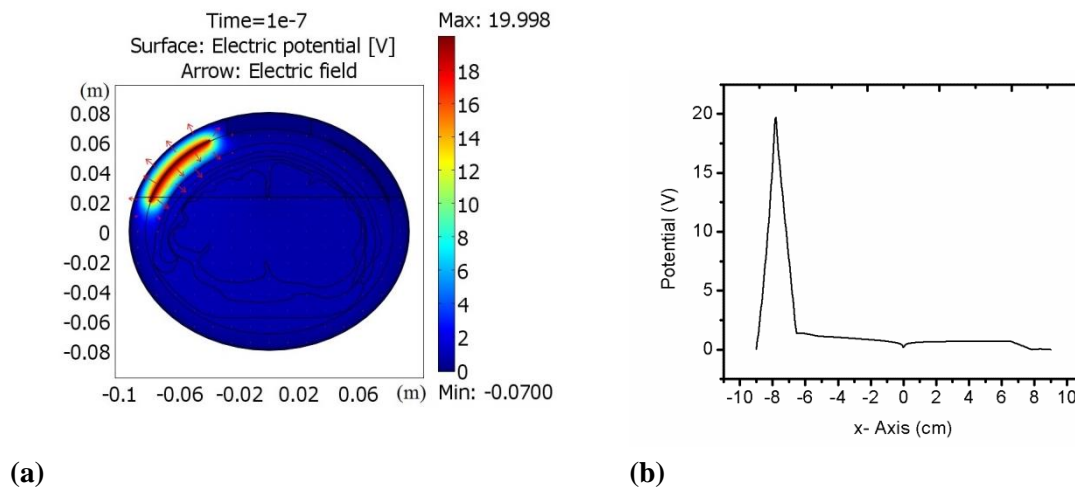


Figure 9. (a) Potential distribution with disturbance at $t = 1 \times 10^{-7}$ s, (b) Profile of potential distribution

Figure 9 (a) is potential distribution in geometry at 1×10^{-7} s. At this time, the signal excitation reaches 20 volt. Figure 9 (b) shows that the potential around excitation electrode is about 20 volt, and potential around detector electrode is about 0 volt. There is a dramatic decline in the potential distribution between excitation electrode position and brain layer position from about 20 volt to approximately 2 volt. Potential in brain layer is about 2 volt and decreasing significantly to -0.07 volt at 0 cm in x-axis where the disturbance potential located. After that, the potential remains stable until it reaches the end of brain layer. The potential backs to 0 volt in detection electrode.

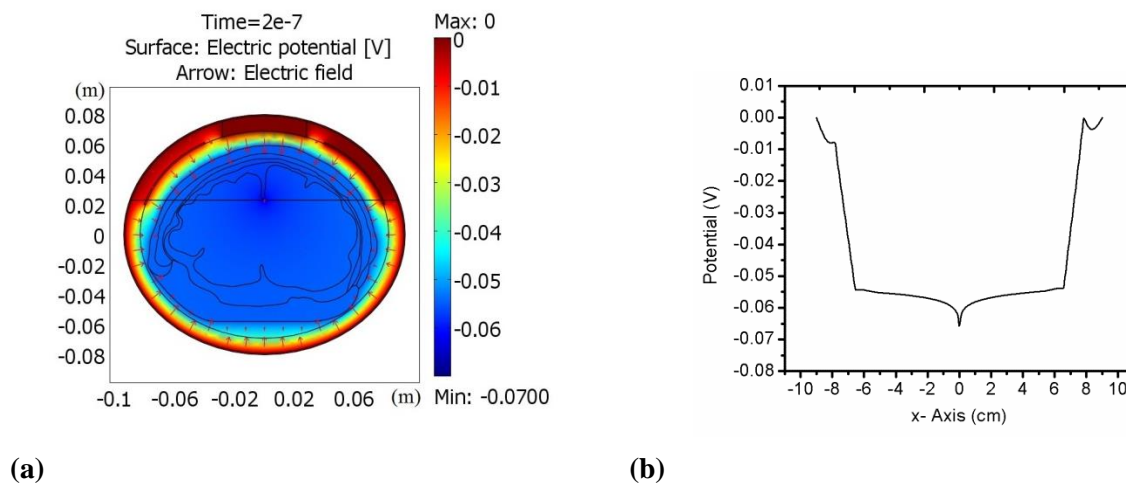


Figure 10. (a) Potential distribution with disturbance at $t = 2 \times 10^{-7}$ s, (b) Profile of potential distribution

Figure 10 (a) is potential distribution in geometry at 2×10^{-7} s. At this time, the signal excitation backs to 0 volt. Figure 10 (b) shows that the potential around excitation electrode is just under -0.01 volt, and the potential around detector electrode is about 0 volt. This potential in brain layer is around -0.055 volt, and it fall slightly to about -0.07 volt at disturbance potential source.

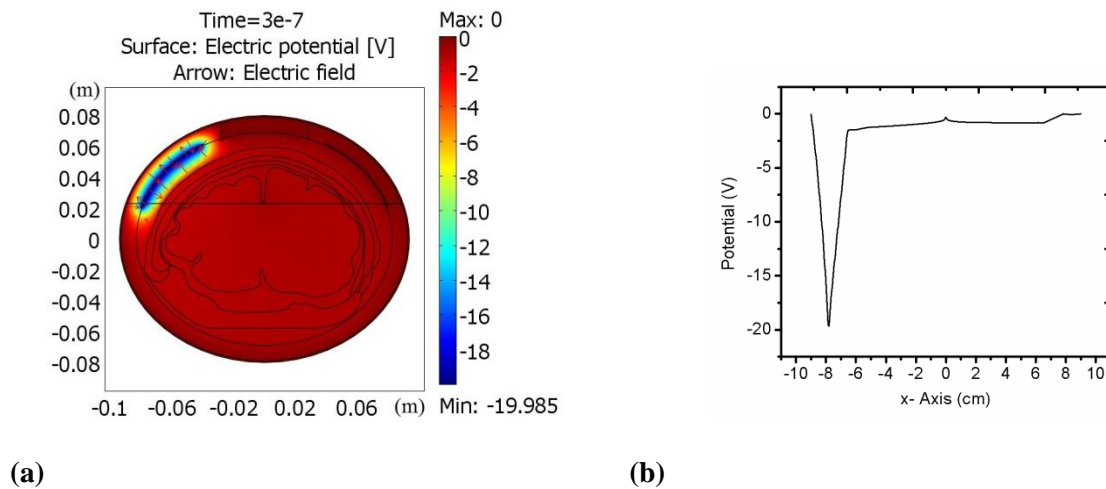


Figure 11. (a) Potential distribution with disturbance at $t = 3 \times 10^{-7}$ s, (b) Profile of potential distribution

Figure 11 (a) is potential distribution in geometry at 3×10^{-7} s. At this time, the signal excitation reaches -20 volt. Figure 11 (b) shows that the potential around excitation electrode is about -20 volt, and potential around detector electrode is about 0 volt. This simulated result looks similar to figure 9. The only difference is the sign oppose each other.

4. Conclusion

In this paper, after solving the governing equation by using finite element method, time dependent potential distribution from non-disturbance potential and disturbance potential of the 2D brain geometry has been generated. There is always a dramatic decrease in the amount of potential distribution at 1×10^{-7} s and 3×10^{-7} s between excitation electrode position and brain layer position in both without disturbance potential and with disturbance potential. However, the physical meaning of these figures needs to be analyzed deeply. In conclusion, there is a noticeable difference between the potential distribution with disturbance and the potential distribution without disturbance.

Acknowledgment

The authors thank Mr. Almushfi of the CTech Labs in Tangerang, Indonesia for assisting the brain design in this study.

References

- [1] Taruno W P, Baidillah M R, Sulaiman R I, Ihsan M F, Fatmi S E, Muhtadi A H, Haryanto F and Aljohani M 2013 *IEEE 10th International Symposium on Biomedical Imaging* pp 1006-9
- [2] Taruno W P, Ihsan M F, Baidillah M R, Tandian T, Mahendra M and Aljohani M 2014 *Middle East Conference on Biomedical Engineering* pp 147-50
- [3] Warsito W, Marashdeh Q and Fan L S 2007 *IEEE Sensor Journal* **7**(4) pp 525-35
- [4] Marashdeh Q, Fan L S and Warsito W 2008 *Ind. Eng. Chem* **47** pp 3708-19
- [5] P T. Ltd 2009 *Operating Manual for the TFLR5000. Electrical Capacitance Tomography (ECT) system* Wilmslow UK, Wilmslow
- [6] Miranda C Pedro, Mekonnen A, Salvador R and Basser P J 2014 *Phys. Med. Biol* **59** pp 4137-47
- [7] The internet resources for the calculations of dielectric properties of body tissues. <http://niremf.ifac.cnr.it/tissprop>. [Accessed February 2015]
- [8] Alme K J and Mylvaganam S 2006 *IEEE Sensor Journal* **6**(5) pp 1256-66
- [9] Banasiak R, Wajman R and Soleimani M 2009 *Insight* **51** pp 36-9
- [10] Liao A, Zhou Q and Zhang Y 2015 *Journal of Applied Geophysics* **117** pp 92-103